Biol. Cybern. 77, 257–266 (1997)

Biological
Cybernetics

# Manuo-ocular coordination in target tracking. I. A model simulating human performance

**Stefano Lazzari**[1], **Jean-Louis Vercher**[2], **Angelo Buizza**[1]

[1] Dipartimento di Informatica e Sistemistica, Università di Pavia, via Ferrata 1, I-27100 Pavia, Italy
[2] UMR CNRS, Mouvement et Perception, Faculté des Sciences du Sport, Université de la Méditerranée CP 910, 163, avenue de Luminy,
F-13288 Marseille cedex 09, France

Received: 6 March 1997 / Accepted in revised form: 15 July 1997

**Abstract.** During eye tracking of a self-moved target, human subjects' performance differs from eye-alone tracking of an external target. Typical latency between target and eye motion onsets is shorter, ocular smooth pursuit (SP) saturation velocity increases and the maximum target motion frequency at which the SP system functions correctly is higher. Based on a previous qualitative model, a quantitative model of the *coordination control* between the arm motor system and the SP system is presented and evaluated here. The model structure maintains a high level of parallelism with the physiological system. It contains three main parts: the eye motor control (containing a SP branch and a saccadic branch), the arm motor control and the coordination control. The coordination control is achieved via an exchange of information between the arm and the eye sensorimotor systems, mediated by sensory signals (vision, proprioception) and motor command copy. This cross-talk results in improved SP system performance. The model has been computer simulated and the results have been compared with human subjects' behavior observed during previous experiments. The model performance is seen to quantitatively fit data on human subjects.

## 1 Introduction

### 1.1 Definition of arm-eye coordination control

During the past 25 years, behavioral, clinical and physiological observations have demonstrated the influence exerted by the arm motor system on the oculomotor system during target tracking tasks. When a human, or a trained monkey, tracks with the eyes a visual target moved by the observer's arm (this condition will be called *self-moved target tracking*), the smooth pursuit (SP) system performance is enhanced, as compared with the condition in which the observer tracks with the eyes an externally driven visual target (*eye-alone tracking*). This was evidenced at the end of the 1960s by Steinbach (1969), who showed that a subject could track a visual target more accurately if the target was attached to the observer's hand. Angel and Garland (1972) attributed this enhanced performance to information transfer between the arm motor system and the oculomotor system. Gauthier and Hofferer (1976a) showed that the interaction between the moving hand and the eyes was preserved even in total darkness: when the observer moved his or her finger and was instructed to track his non-viewed fingertip with his eyes, SP could be produced without vision, though with lower gain than in experiments where the finger was visible. On the contrary no SP movements could be produced during the tracking of either imaginary or acoustic targets in the dark (Gauthier and Hofferer 1976b; Buizza et al. 1979).

In order to interpret this behavior, Gauthier et al. (1988) introduced the notion of an intersystem temporal control, defined as *coordination control*. According to this hypothesis, the coordination control would result from an exchange of sensory and motor information between the arm motor system and the SP system when they are involved together in a common task, e.g. tracking a visual target. Thus, the coordination control would combine and interact with the basic control of each (eye and arm) motor system taken in isolation. The putative model proposed by Gauthier et al. (1988) characterized the coordination control in terms of improvement in *timing* and *mutual coupling*. The timing aspect accounted for the fact that SP latency is shorter when the eyes follow the observer's finger than when they track an external target. The mutual coupling accounted for the changes in the static and dynamic behavior of the SP system (increased maximum velocity, frequency limit and accuracy).

### 1.2 Nature and respective role of the signals

The nature of the nonvisual signals responsible for coordination control has long been debated. Steinbach (1969) demonstrated that subjects showed better visual tracking of a target attached to their *actively* moved arm than *passively*. Based on this evidence, Steinbach proposed that SP enhancement was due to the arm motor efference. Gauthier and Hofferer (1976a) suggested that inflow from the moving finger

---

*Correspondence to*: J.-L. Vercher (Tel: +33 4 91 17 22 62,
Fax: +33 4 91 17 22 52, e-mail: vercher@laps.univ-mrs.fr)

was necessary to trigger SP in total darkness: inflow suppression by an ischemic block applied to the arm prevented self-moved imaginary target tracking even if the finger was actively moved. Gauthier and Mussa-Ivaldi (1988) showed that section of the dorsal roots innervating the arm of trained monkeys produced the same dramatic effects on motor control of the ipsilateral arm as in previous experiments with deafferented monkeys (Knapp et al. 1963; Lamarre et al. 1978) but also produced specific effects on eye-arm coordination (lower SP gain, higher number of saccades, lower maximum velocity during self-moved target tracking) without affecting eye-alone tracking performance. After surgery, the ability to produce in darkness slow eye tracking in response to the motion of the ipsilateral arm disappeared, but SP latency during tracking of a target attached to the contralateral arm was still short. Following Gauthier et al. (1988), one may suppose that both efferent and afferent signals are needed to improve SP tracking of an arm-attached target.

It has recently been confirmed that the arm motor command is responsible for the short latency between the arm and the eye motion onsets, while arm proprioception plays a role in the changes in the SP characteristics observed when the subject tracks his own arm (Vercher et al. 1996). This was done by comparing the performance of control subjects tracking their passively moved arm with the performance of patients without proprioception, tracking their actively moved arm. In brief, when control subjects track with their eyes their passively moved arm, the SP latency is as long (125 ms) as when tracking an externally moved target (130 ms). When deafferented subjects track their actively moved arm, SP latency is as short (−8 ms) as is observed with control subject in the same task (−5 ms). This shows the role of the arm motor command in eye-arm timing control. In the self-moved target tracking condition, accuracy, maximum velocity and frequency limit are lower in deafferented patients than in control subjects, showing a probable role of arm proprioception in mutual coupling.

To assess the descriptive model of coordination control introduced by Gauthier et al. (1988), in the present paper we introduce a quantitative model of the manuo-ocular coordination control system. This model can produce realistic arm and eye trajectories in the horizontal plane, and can simulate the parametric (static and dynamic) changes occurring in the oculo-manual system when the two subsystems perform concomitant tasks. A qualitative comparison between the model and human performance, based on arm and eye trajectory patterns, is presented in a companion paper (Vercher et al. 1997).

We know of no other model with these characteristics. Previous studies of coordination between arm and eye tracking systems have been done at an analytical level only (Miall et al. 1985, 1988; Steinbach 1969), and the models proposed were either purely descriptive (Gauthier et al. 1988) or very schematic (Bock 1987).

## 2 Model structure and experimental conditions

Our goal was to create, on the basis of the previous studies reported above, a model able to perform accurate oculo-manual tracking while keeping a high level of parallelism with the structure of the physiological system. For this purpose, we implemented a model composed of three interacting subsystems (Fig. 1): an eye tracking system, an arm motor system and a coordination control system. The model of the eye tracking system combines a SP branch, correcting for the retinal slip, and a saccadic branch, correcting for the retinal error. The SP branch has been developed on the basis of models proposed by Young (1971) and Robinson et al. (1986). For the saccadic branch, although many models have been proposed with different levels of sophistication (Robinson 1975; Becker and Jurgens 1979; van Gisbergen et al. 1981; Young 1981), we considered a simplified model based on the scheme presented by Young and Stark (1962). In fact, only the existence, the time of occurrence and the accuracy of the saccadic components in the tracking were relevant to our purpose, while details about their generation were not. The arm motor branch is derived from the model proposed by Stein et al. (1987).

The most original feature of the model is represented by the *coordination control system (CCS)*, which receives signals from the two motor systems and accordingly changes the dynamics of the SP branch. Changes concern both timing (e.g., the synchronization between the target, the arm and the ocular movements) and mutual coupling (e.g., the exchange of information between the two systems). As shown by computer simulation, the CCS allows the model to correctly reproduce the typical behavior of eye and arm subsystems when stimulated alone and the typical changes of SP performance during self-moved target tracking. In both qualitative and quantitative aspects, the model closely fits the performance of human subjects submitted to tracking tasks, as previously described in the literature (Gauthier et al. 1988; Vercher and Gauthier 1992; Vercher et al. 1993, 1995, 1996).

Three tracking conditions were considered: eye-alone tracking (EAT), where the subject follows an external target with the eyes only; eye and hand tracking (EHT), where the subject follows the external target with both the eyes and the arm; and self-moved target tracking (SMT) where the subject moves the target with his hand, sinusoidally, at a learned amplitude and frequency and tracks the self-moved target with his eyes. More details about the experimental protocols used with humans are given in other papers (Vercher et al. 1993, 1995, 1997).

## 3 Model implementation

As already stated, the model (Fig. 1) contains three parts: the arm motor system, the oculomotor system and the CCS. The model mostly addresses the sensory and motor control structures at the level of the central nervous system (CNS). The peripheral properties of the arm and the eye plants are represented and modelled through transfer function blocks $G(s)$ that summarize the dynamics properties (mass and viscoelastic characteristics) of the plants. The following transfer functions have been chosen to represent the mechanics of the arm and the eye plants (bones, muscles and tissues), respectively. The model parameter values are physiologically plausible and based on data found in the literature.

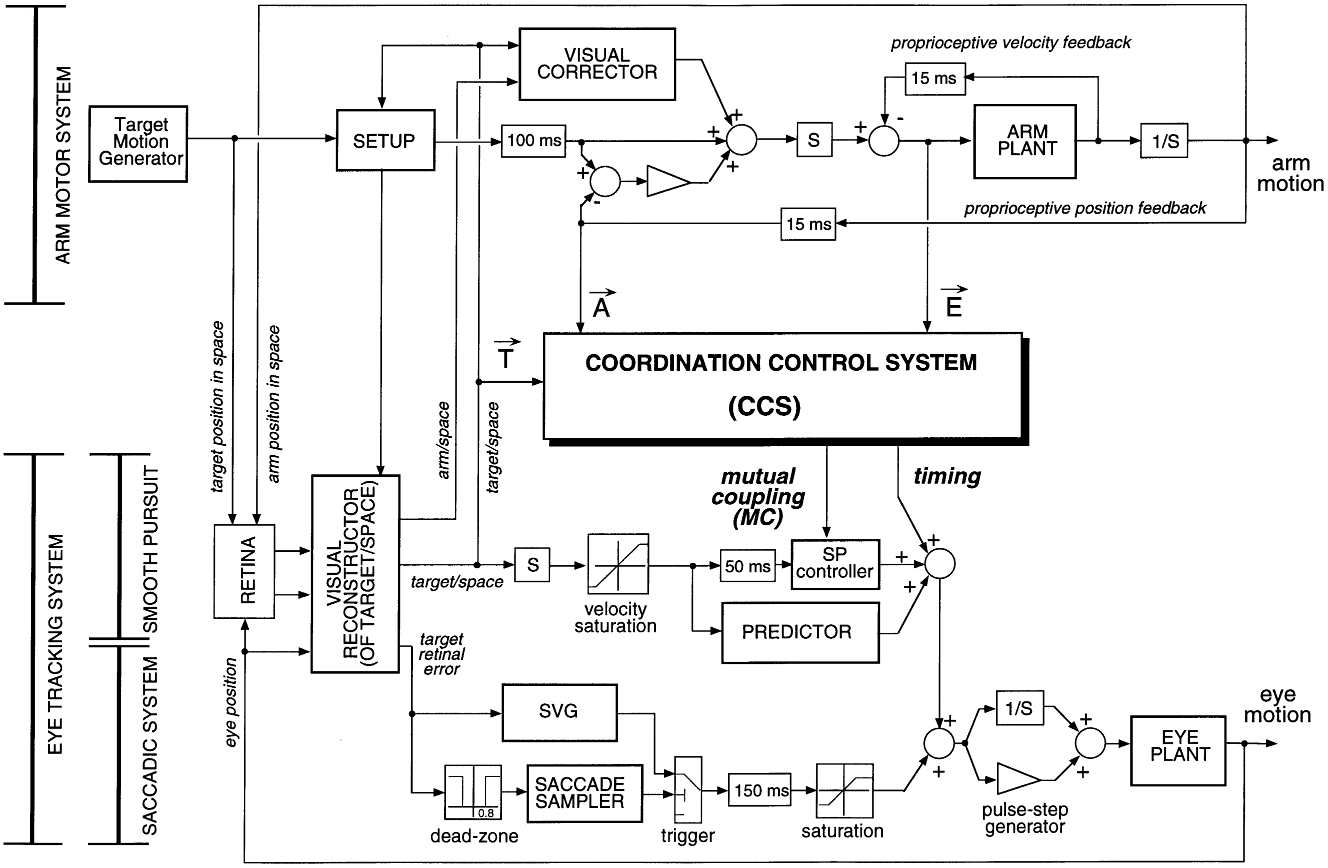

**Fig. 1.** Block diagram of the model. The *lower part* shows the eye tracking system, with the saccadic branch and the smooth pursuit (SP) branch. In the *upper* part is the arm motor system. At the *center* is the coordination control system, controlling the exchange of information between the two sensory-motor systems. The *circles* represent additive or subtractive operations. The *triangles* are gain (multiplicative) elements. The Laplace notation is used, the $s$ operator denoting a derivation while the $1/s$ operator denotes an integration. See text for details on the other blocks

$$K/(s^2 + 2\xi\omega s + \omega^2) \quad \text{with } K = 70\ , \quad \omega = \sqrt{20}$$

$$\xi = 7/\sqrt{20} \quad \text{for the arm plant} \tag{1}$$

$$A/(s + B) \quad \text{with } A = B = 20/3 \quad \text{for the eye plant} \tag{2}$$

### *3.1 Peripheral components*

The common input source is the *target motion generator (TMG)*, providing the input signals to the different parts of the model. In the EAT and EHT conditions, it represents an external target generator, providing sinusoidal target position signals at different frequencies and amplitudes. In the SMT condition, it represents the subject's 'intention' to perform a specific movement and generates a cos-bell position wave, replicating the single movement produced by human subjects during the SMT condition.

The *setup* block allows the selection of the desired condition (either EAT, EHT or SMT) and sends the appropriate input signals to the eye and the arm systems. Namely, in the EAT condition the input to the eye system is the external signal produced by the TMG, while the input to the arm system is zero. In the EHT condition, both eye and arm systems receive the same input, i.e. the target motion generated by the TMG. Finally, in the SMT condition, the input to the arm system is an 'internal' signal (the intention of moving the arm), and the input to the eye system is the arm position signal (i.e., the output of the arm motor system), which also represents the self-moved target position.

The oculomotor part of the model contains two branches: the SP branch and the saccadic branch. They are mostly independent of each other, except that they share the same input (from the *visual system*) and output (pulse-step generator and motor plant). In order to keep a parallelism with the physiological system, which mostly uses target velocity as input signal to the SP branch and retinal error as input to the saccadic branch, the *visual reconstructor* supplies the saccadic branch with the retinal position error and the SP system with target position in space. Target position in space is reconstructed as the sum of retinal error and a reafference of eye position in the head, as in Robinson et al.'s (1986) model. The output of the overall eye tracking system represents the eye position relative to the head (i.e., in space since the head is still) in the horizontal plane.

### *3.2 Visual elements*

Input signals to the oculomotor system come from both the retina and the visual reconstructor. These two blocks play the role of pre-processing the incoming visual signals coding arm ($A$), target ($T$) and eye ($E$) position. Both use only arithmetic sum operators. The retina computes the positional errors of eye versus target ($Err_{et} = T - E$) and arm versus target ($Err_{at} = A - E$) and sends them to the *visual reconstructor*. Here they are added to an extraretinal eye position signal ($E'$) to provide the estimated positions of the target ($T' = Err_{et} + E'$) and of the arm ($A' = Err_{at} + E'$) in space. Robinson et al. (1986) used an internal model of the eye plant to refine the estimated eye position. This level of sophistication did not seem necessary here. Depending on the experimental condition, either $Err_{et}$ or $Err_{at}$ is transferred to both the saccadic branch and the SP branch. At the input of the latter, the position signal is differentiated to compute target velocity in space, which is assumed to be the driving input to the SP system.

The *visual reconstructor* also supplies target position to the *arm motor system* and to a *visual corrector system*. The last provides a signal compensating for the error between the arm and the external target positions (see below). These operations introduce an overall delay of about 50 ms, identified as the sensory delay of the visual system (Kawano et al. 1990).

### 3.3 Saccadic branch

In the simplified model of the saccadic system implemented here, the retinal error $Err_{et}$ coming from the visual reconstructor is used as input signal. A *dead-zone* limits to 0.8° the smallest retinal error for which saccades are generated (Becker 1989). In order to account for the well-known fact that a saccade cannot immediately be followed by another, a sampler block imposes a refractory period between two consecutive saccades (200 ms), i.e., an interval after a saccade, in which no other saccade can be triggered (Jurgens et al. 1981). In parallel with these blocks, whose role is actually to trigger a saccade, the *saccade velocity generator (SVG)* computes the intended saccade velocity ($SV$) based on $Err_{et}$ and its derivative (Robinson and Keller 1972):

$$SV = 25^{*}Err_{et} + 4^{*}\mathrm{d}(Err_{et})/\mathrm{d}t \tag{3}$$

The coefficient values were determined empirically, by evaluating the saccade accuracy in tracking sinusoids with different amplitudes and frequencies.

The SV is passed through a 150-ms delay block, accounting for the specific latency of the saccadic system (Westheimer 1954). Finally, saccade velocity is limited to 800°/s (Bahill and Stark 1979) by a saturation element.

### 3.4 SP branch

The SP branch is directly inspired by Young's (1971) model. In that model an internal positive feedback loop compensates for the visual (negative) feedback. In this way SP actually works in open loop thus avoiding any instability problem, in particular those related to the presence of delays in a closed loop. This scheme has been proposed in many successive models, though with several adjustments (e.g., Bahill and McDonald 1983; Robinson et al. 1986). In our model, the visual reconstructor plays the same role as the internal feedback loop in Young's (1971), Bahill and McDonald's (1983) and Robinson et al.'s (1986) models; actually it is in charge of opening the loop by adding the retinal and the eye position signals. Target-in-space velocity, bounded to an upper limit of 100°/s (velocity saturation block), is sent to two parallel blocks: the *SP controller* and the *predictor*. The role of the predictor is to compensate for the delay due to both the visual (50 ms) and the SP systems (40 ms). The predictor on-line forecasts target velocity for the next 400 ms, on the basis of a cubic spline interpolation of the actual target velocity during the last 150 ms. The estimated velocity is limited to 110% of the maximal target velocity in order to avoid unrealistic estimations of target accelerations. The relative contribution (gain) of the predictor to the SP branch has been set to 0.36, while the SP controller has been assigned a dc gain of 0.93 and a pole at 1.22 Hz. This parallel structure is not unlike the structure proposed by Bahill and McDonald (1983) in their 'Target Selective Adaptive Controller' model. The difference between that model and the one proposed here is that in the former, prediction relies on the existence of a 'catalog' from where the trajectory to be tracked is chosen, based on the actual target movement, whereas in our model prediction is based on on-line extrapolation of target motion.

The output of the saccadic branch and the SP branch are summed and sent to the pulse-step generator, which provides the motor command to the eye plant. The eye plant transfer function is given by (2). The output of the eye tracking system is eye position in the head (i.e., in space, since the head is still). It should be stressed once again that the goal of this visuomotor branch model is to provide a simple tool for simulating visuomotor behavior in order to study eye-hand interaction and coordination, and not to study visuomotor behavior per se. In this sense it seemed justified to introduce some simplifications that would not be acceptable in a different context and to use simplified models, provided they are able to generate realistic eye movements.

### 3.5 Arm branch

As opposed to the eye tracking system, we failed to find in the literature a reference model for the arm tracking system. Most of the models published recently concern rapid arm movements, e.g., simulating pointing movements. We then designed a very simple model in which the intended arm movement (position) is delayed by 100 ms (e.g., the central processing delay; Jones and Hunter 1990; Cordo et al. 1994), differentiated and sent to the arm motor plant. Input signals are provided by the *visual reconstructor* of the target position and through a *visual corrector*, which provides a signal compensating for the positional error between the arm and an external target.

The arm control system has been provided with two feedback loops (velocity and position). The relevant signals represent proprioceptive information and include the overall somatosensory information related to joint posture and kinematics (Cordo et al. 1994). Two loops were considered for the sake of clarity, though it is known that the afferent fibers simultaneously carry position and velocity information to the CNS (Sittig et al. 1985). Both loops have a delay of 15 ms (Lamarre et al. 1983; Cordo et al. 1994). The stability of the arm subsystem has been tested and verified for different delay up to 200 ms at least. This states for a large phase margin when a delay of 15 ms is used, as in our simulations. The output signal from the arm branch is the arm position, i.e., the angle of the elbow joint.

### *3.6 Visual error correction*

The above arm motor system model cannot exhibit a known property of the human arm tracking system, which seems to behave like an intermittent servo-controller. In fact, the tracking of a slowly moving target is performed with a sequence of single, fast movements instead of a continuous movement (Craik 1947; Navas and Stark 1968). This intermittency is attributed to visual correction of arm trajectory (Miall et al. 1993). In our model, visual correction of arm movement is controlled by a block whose structure and implementation are inspired by results from John Stein's group (Miall et al. 1988, 1993; Stein et al. 1987; Wolpert et al. 1992). The *visual corrector* computes the visual retinal error between the arm-attached target and the external target position and, through a PID controller, provides the arm branch with a correcting signal that allows the system to reach zero position error at steady state. The PID controller has both the proportional and the integral terms equal to 2. The presence of the integral term assures stability of the arm system and zero position error at steady state. According to the experimental evidence, correction is prevented when target velocity exceeds 40°/s (e.g., in concomitance with target jumps that would induce fast arm movement without visual correction) and the minimal error between arm and target is less than 0.3° (Wolpert et al. 1992).

### *3.7 Coordination control system*

The coordination control system (CCS) (Fig. 2) is the central part of the model. The CCS controls the signal exchange between the eye and arm subsystems. It is made up of two main parts. The goal of the first (top of Fig. 2) is to change the dynamics of the SP system when the arm motion in space and the target motion in space are correlated (e.g., when the target is moved by the observer's hand). To achieve this, the block receives as inputs the target position in space ($T$) from the *visual reconstructor* and the arm position ($A$) from arm proprioception, computes their auto- and cross-correlation and, depending on their values, changes the dynamic of the SP controller. A 25-ms delay is applied to $A$ and adds to the 15-ms delay in the proprioceptive position feedback in order to take into account the visual delay of 40 ms introduced in reconstructing $T$ and synchronize $A$ and $T$. The cross-correlation and auto-correlation of $T$ and $A$ are used to compute the following parameters, where the dimension of the vectors $T$ and $A(m)$ is set so as to correspond to a time interval of 150 ms:

$$\alpha = \max_{-m+1<\tau<m-1} \left\{ f(\tau) = \sum_{k=1}^{m} T(k)A(k+\tau) \right\}$$

$$a = \max_{-m+1<\tau<m-1} \left\{ f(\tau) = \sum_{k=1}^{m} A(k)A(k+\tau) \right\}$$

$$b = \max_{-m+1<\tau<m-1} \left\{ f(\tau) = \sum_{k=1}^{m} T(k)T(k+\tau) \right\}$$

$$\text{with} \quad \begin{matrix} m = 30 \text{ (equivalent to 150 ms)} \\ \tau \in N \end{matrix} \tag{4}$$

$$\beta = \max\{a, b\} \tag{5}$$

The ratio $\alpha/\beta$ is then computed and used to determine the *mutual coupling (mc)* signal:

$$\begin{cases} \text{if} \quad \dfrac{\alpha}{\beta} \geq 0.8 \quad mc = 0 \\ \text{if} \quad \dfrac{\alpha}{\beta} < 0.8 \quad mc = 1 \end{cases} \tag{6}$$

This signal is used to change the SP controller dynamics, according to the equation

$$SP_c(s) = \frac{0.93}{0.021(1 + 5.5\,mc)s + 1} \tag{7}$$

Notice that when arm and eye movements are strongly correlated ($\alpha/\beta \geq 0.8$) then $mc = 0$ and the time constant of $SP_c(s)$ is low (0.02 s), whereas this is high (0.13 s) when the movements are weakly correlated ($\alpha/\beta < 0.8$ and $mc = 1$). The values of these two time constants have been set by fitting model simulation to the data presented by Vercher et al. (1993). Slightly different values (e.g., in the intervals [0.015, 0.025] and [0.11, 0.15] respectively) will change only the position of the poles in the frequency response of the SP system (Fig. 3B) without affecting the stability of the overall system.

In the EAT condition, the arm is motionless, the cross-correlation between $A$ and $T$ is zero and $\alpha$ is equal to zero. The mutual coupling signal is then 1 and the SP *controller* transfer function is $SP_c(s) = 0.93/(0.13s + 1)$ as introduced in Sect. 3.4. In the EHT condition, both the eye motor system and the arm motor system receive their input signal from the *visual reconstructor*. Due to the 15-ms delay introduced by the proprioceptive position feedback and the 25-ms compensating delay applied to $A$, the two signals are shifted and are only slightly correlated: $\alpha$ is low, $mc = 1$ and the SP controller transfer function does not change. Finally, in the SMT condition, system delays make the signals $T$ and $A$ strongly correlated, leading to a high value of the $\alpha/\beta$ ratio, a mutual coupling signal equal to 0 and SP controller transfer function $SP_c(s) = 0.93/(0.02s + 1)$.

The second part of CCS (bottom of Fig. 2) plays a role only in the SMT condition, where it multiplies the input signal, represented by the arm motor command ($E$), by a smoothing function and provides a signal (*timing*) to the SP system, which allows it to overcome the 130-ms initial delay. The absolute value of the efference motor command ($E$) is first integrated, $x = \int |E| \mathrm{d}t$, and then multiplied by a smoothing function whose independent variable is represented by the integrated efference itself. Smoothing has been introduced to limit in time the influence of the arm efference copy on SP as a function of the frequency of the target motion. The smoothing function $G(x)$ has been determined empirically:

$$\textit{Timing} = x \cdot G(x) \quad \text{where } G(x) = \frac{25 - x}{0.2x^7 + 400} \tag{8}$$

Since $x > 0$ and monotonically increases for $t > 0$ and for each motor signal $E$, it is easy to show that $G(x)$ is a

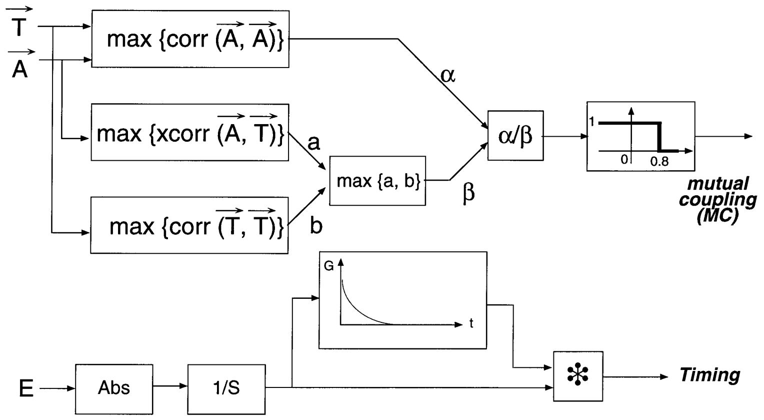

**Fig. 2.** Block diagram of the coordination control system (CCS) model. The block has three inputs: the reconstructed position of the visual target ($T$) to be followed by the SP system, the arm position through proprioception ($A$) and the arm motor command ($E$). The outputs of the CCS act on both the SP controller (mutual coupling, $mc$), and the triggering of the SP (timing). See text for details

$C^1$ function whose absolute value rapidly tends to zero as $x$ increases above the value of about 5 (e.g., $|G(x)| < 10^{-5}$ for $x > 10$ and $|G(x)| < 10^{-6}$ for $x > 15$, etc.). Moreover $G(x)$ varies in a continuous and regular way when changing coefficients in (8). A change in parameter values would not influence either the performance or the stability of the overall system, but would introduce undesired corrective saccades.

The underlying idea is that the intention to move the eyes and the arm together makes a copy of the arm motor command available to the SP system so that arm and eye movements may start at almost the same time. The smoothing function limits the effect of this coupling to a short period after movement onset. In this sense it may correspond to a kind of short memory mechanism.

## 4 Quantitative evaluation

### 4.1 Modelling and simulation tools

The model has been designed and simulated using Matlab with Simulink (The MathWorks, Inc.) running on a PC, Windows-based platform (Pentium 133 MHz, 16 Mb RAM). The model was drawn using the Simulink graphical interface and integrates some Matlab functions (M files). During the simulations of EAT and EHT conditions, the model input signal, depicting the target motion in space, was a sinewave (peak-to-peak amplitude 20°, frequency 0.1–2.0 Hz). In the SMT condition, the input signal (position) has been chosen to be $[15\sin(2t - \pi/2) + 15]$ in the time interval $[0, \pi]$ to allow comparison with the arm movement produced by subjects, i.e., a sinusoidally shaped signal, with position and velocity equal to zero at onset and offset.

### 4.2 Data analysis

The quantitative evaluation of the model's performance was based on harmonic analysis (Vercher et al. 1993). To calculate the SP gain, saccades were first removed from eye movement. Saccades were detected using an acceleration threshold, were removed from the eye velocity curve and replaced by the average velocity of the SP component just before and after the saccades. The gain of the SP system was computed for each target motion frequency as the ratio of the peak value of the power spectral density of the eye motion signal and the peak value of the power spectral density of the corresponding target motion signal.

### 4.3 SP latency: timing

Most of previous work on arm-eye coordination is based on the analysis of SP latency changes in different experimental conditions. With the dynamic blocks and internal delays set as above, the simulations showed that the response of the SP system to an external visual target (condition EAT) presented an onset latency of 120 ms while in the SMT condition, the eye-to-arm latency was $-5$ ms. These values may be compared with the average latencies observed with human subjects in previous studies (for instance, Vercher et al. 1996 showed latencies of $150 \pm 29$ ms and $-5 \pm 35$ ms in the EAT and SMT conditions, respectively). This result stems from the contribution of the arm motor command to the eye movement control via CCS. It is worth recalling that SMT condition improves the onset of the oculomotor response by reducing its latency, but apparently does not affect at all the way the eye movement ends. In fact when the self-moved target stops the eye movement shows the same pattern as during EAT tracking and one or two resetting saccades are observed before the pursuit velocity declines to zero. This may be viewed as supporting the hypothesis that eye-arm interaction has no effect on SP prediction.

### 4.4 Changes in SP bandwidth: mutual coupling

Another crucial feature of coordination control as defined by Gauthier et al. (1988), together with the timing aspects (see above), is the mutual coupling that is responsible for the increased performance of the SP system when the visual target is directly attached to the observer's moving arm. Mutual coupling has been characterized as an increase in the maximum velocity of the SP system response in the SMT condition as compared with EAT (Gauthier et al. 1988), and an increase in the bandwidth of the SP system (Vercher et al. 1993). Gauthier et al. (1988) used target ramps (constant-velocity target movement) and single arm movements, while Vercher et al. (1993) used sinewaves. In EAT in similar conditions, Buizza and Schmid (1986, 1989) showed that the saturation level of the SP response velocity depends on the amplitude of target motion and interpreted this result as

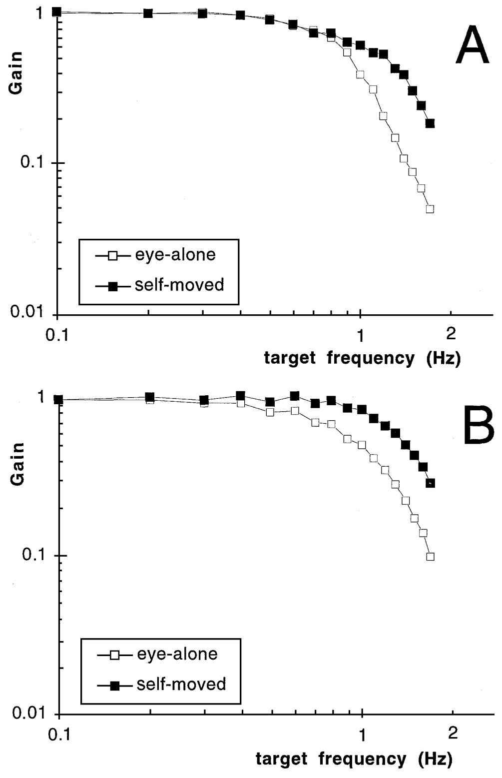

**Fig. 3. A** SP velocity gain versus frequency in response to an external target (EAT condition: open squares) and in response to a self-moved target (SMT condition: *filled squares*). The values are mean data obtained from five human subjects (from Vercher et al. 1993). **B** Results of model simulation from the same experimental conditions as in **A**. See the text for details

depending on the dynamics of the SP system. These data suggest that the increased maximal velocity (Gauthier et al. 1988) and the increased bandwidth (Vercher et al. 1993) in SMT as compared with EAT may be due to a common cause, and depend on the dynamic behavior of the overall tracking system, since increasing the target motion frequency while maintaining the amplitude, or changing the amplitude at constant frequency, lead to similar changes in target motion maximum velocity. We imagined two possibilities for this mechanism, both assuming that the velocity saturation of the SP system is of about 100°/s (Meyer et al. 1985) and is located upstream from the SP motor system, i.e., in the visual system: (a) the coordination signal brings a contribution to the eye motor command at the level of the visual reconstruction system (downstream from the saturation) or (b) the coordination signal acts on the SP controller itself. Although it is difficult to find the exact anatomical equivalent of the model elements, the former hypothesis is more consistent with the assumption that the coordination takes place at the cortical level (areas MT and MST, where the reconstruction of the movement of the target re space takes place: Newsome et al. 1988), and the latter hypothesis is more consistent with the assumption that coordination is performed at the cerebellar level. Previous experience shows that cerebellar lesions produce effects on SP similar to a change of bandwidth (see, for instance, Zee 1986; Suzuki and Keller 1988). We tested the latter hypothesis on the model by making the CCS change the frequency response of the SP controller whenever the eye motor system is tracking the arm motor system [see (7)]. The signals involved in this modification are the target reconstruction in space ($T$) coming from the visual reconstructor, and the arm position ($A$) from the proprioceptive feedback (Fig. 2).

The dynamical performance of the model has been tested in EAT and SMT conditions, while the target was moving at different frequencies ranging from 0.1 to 1.7 Hz over constant peak-to-peak amplitude (20°). A comparison of the model and the performance of human subjects is given in Figs. 3 and 4. Data from human subjects were taken from Gauthier et al. (1988) and Vercher et al. (1993) for the velocity and frequency domains, respectively. Model simulations have been obtained by inputting a sine or a triangular wave at different frequencies and amplitudes into the arm motor system. The eye motion signal was processed in the same way as for the human subjects, as described in Vercher et al. (1993).

Figure 3 shows the gain of the SP system as a function of target motion frequency in the range 0.1 Hz to 1.7 Hz over an amplitude of 20°. Average data from human subjects (Fig. 3A) are taken from Vercher et al. (1993) who tested five subjects in the two tracking conditions (EAT and SMT). The −3 dB frequency cut-off of the SP system frequency response was at 0.75 Hz in EAT, and 1.0 Hz in SMT. When the target was moving at a frequency of 1.7 Hz, the SP gain was 0.05 in EAT and 0.19 in SMT. Vercher et al. (1993) reported that the performance increased in SMT for all subjects, as compared with EAT, this increase being either evidenced in terms of gain or in terms of phase shift, depending on the subject. The simulation showed similar effects of the tracking condition on the gain curves (see Fig. 3B).

### *4.5 Changes in SP velocity saturation: contribution of arm proprioception*

Figure 4 shows the static relationship between the higher target velocity during a trial and the corresponding maximal eye velocity. The highest SP velocity and the range of linearity of the SP system have long been debated. Rashbass (1961) reported that the maximal velocity was close to 40°/s. Buizza and Schmid (1986) showed that the SP maximal velocity depends on the target motion path and amplitude, resulting in a saturation of the response which depends on target motion amplitude. These authors recorded SP velocities up to 64°/s when the target followed a sinusoidal path with peak-to-peak amplitude of 50° and frequency of 0.48 Hz, corresponding to a gain of 0.86. Meyer et al. (1985), using constant-velocity ramps of target movement showed that humans can produce SP eye velocity up to about 100°/s if the amplitude and duration of target motion are large enough to allow SP response velocity to reach steady state. This proves that the saturation level of the SP system in humans is at least 90–100°/s. Mean data, obtained with human subjects, taken from different authors are presented in Fig. 4A. The target motion was periodic, with either sinusoidal (Vercher et al. 1993) or square wave velocity profiles (Buizza and Schmid 1986; Gauthier et al. 1988), and peak-to-peak amplitudes of 10° and 50°, respectively. Data obtained from sinewaves

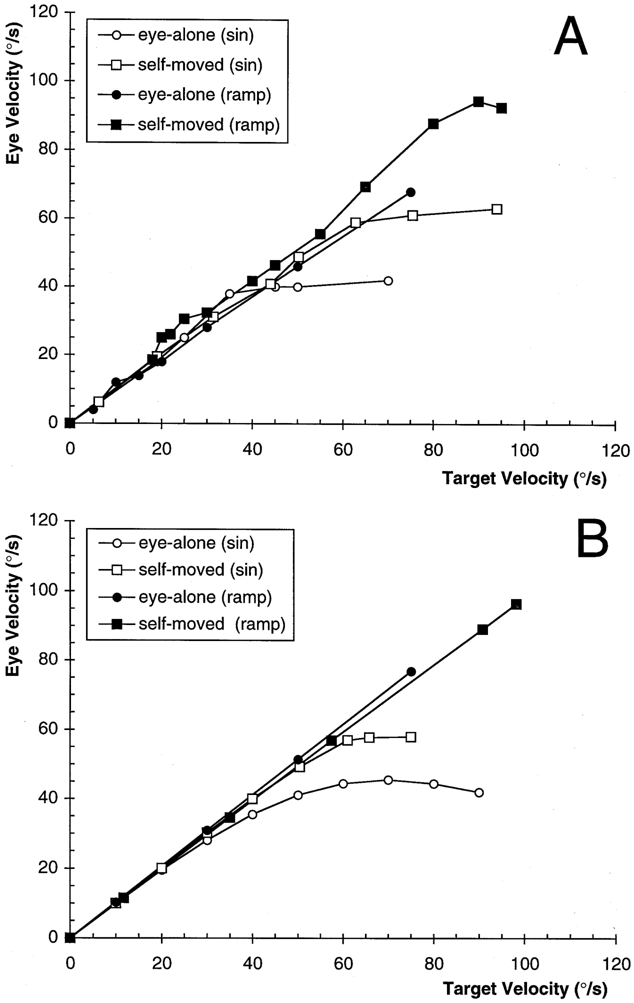

**Fig. 4. A** Relationship between target velocity and SP eye velocity in two tracking conditions (EAT, *circles*; SMT *squares*) in five human subjects. Two types of target motion are used: triangular waves (T-waves), i.e., square waves of target velocity, with peak-to-peak amplitude of 50° (*filled symbols*) and sinewaves (S-waves) with peak-to-peak amplitude of 20 (*open symbols*). Data are from Buizza and Schmid (1986) (EAT with T-waves), Gauthier et al. (1988) (EAT and SMT with T-waves), and Vercher et al. (1993) (EAT and SMT with S-waves). **B** Results of model simulation for the same conditions as in **A**

(S-waves) are represented with open symbols while data obtained from square waves (i.e., triangular position waves, T-waves) are represented with filled symbols. In the EAT condition (circles), the SP velocity saturated at about 40°/s with S-waves, and reached 60°/s with T-waves. In the SMT condition (squares), the SP velocity saturated around 60°/s with S-waves and matched the target velocity up to 100°/s with T-waves.

Figure 4B shows the simulation results. To allow comparison with the data from humans, the two types of target motion (S- and T-waves) were given the same characteristics as in the experiments: S-waves with a peak-to-peak amplitude of 20° and T-waves with peak-to-peak amplitude of 50°. The test frequencies allowed peak target velocities between 10°/s and 100°/s to be obtained. Due to the slow dynamics of the arm plant, it was not possible to maintain the amplitude of the arm motion during high-frequency sinusoidal target motions and thus the arm model failed to reach high velocities (the dynamics of the arm plant had been set for slow movements). Simulation results are very similar to human data. In the EAT condition, the simulated SP velocity saturated at about 44°/s using S-waves, while it reached 76°/s with T-waves; in the SMT condition the SP velocity saturated at about 58°/s with S-waves and reached maximal velocities up to 96°/s with T-waves. In conclusion, as in the study by Buizza and Schmid (1989) the lower velocity saturation observed in some experimental conditions is interpreted as a consequence of the dynamic behavior of the SP system when exposed to small-amplitude target motions.

## 5 Conclusion

Behavioral studies with human subjects, conducted over the last 10 years, provide us with a better understanding of the mechanisms and the signal flow subserving the coordination between the arm motor system and the oculomotor system when both systems are involved in a self-moved target tracking task. In the present paper we have presented a possible model for these mechanisms. The model structure is based on the hypothesis of the existence of a *coordination control system (CCS)* originally proposed by Gauthier et al. (1988). The CCS is assumed to be active during concomitant movements of eye and arm, and to influence both the timing and the dynamics of the SP system. The model proposes a formal representation of these interactive mechanisms based on the idea that a motor command copy of the arm, an afferent signal from arm proprioception, which codes arm position, and a target-in-space signal reconstructed from visual input are all made available to the CCS and used to reduce the initial SP movement latency and to widen the SP pass-band.

Because the main goal of the study was to test the plausibility of the CCS hypothesis, the oculomotor system and the arm motor system are represented in a rather simplified way. Minimal models have been chosen, able to reproduce the main patterns of behavior of the two motor systems. In particular, an open-loop scheme has been adopted to represent the SP control system, based on Young and Stark (1962), in order to avoid the stability problems raised by the presence of delays in closed-loop models. The use of more sophisticated representations would perhaps increase the realism of the model, but would not have any influence on the interaction mechanisms. Though it is clear that presenting a model which works well does not prove that it correctly reproduces the physiological reality, the model does help to test hypotheses and to reject them when model predictions do not fit the behavioral observations. From this point of view, the present model seems to prove that coordination control based on integration of visual, (pre)motor and proprioceptive signals is a tenable hypothesis in eye-arm movement coordination. In this sense, the model we have proposed may also help guide the experimental research on the physiological mechanisms and anatomical sites involved in coordination. A more thorough evaluation of the model by comparison between experimental and simulated responses is proposed in the companion paper (Vercher et al. 1977) and shows that the model is able to simulate human behavior closely, even when the normal visuo-manual relationship is artificially altered.

Further developments of the model are planned in order to introduce more realistic peripheral components (arm and eye motor plants, taking into account the real biomechanical properties of the arm and the eyes, and the closed-loop structure of the SP system). Moreover, it is evident that a comprehensive model should also display adaptive and learning capabilities. The use of internal representation of the controlled plant has been proposed by several authors as a way for the CNS to take into account the properties of the peripheral systems, and to overcome the internal delays due to neural transmission and processing time (Gerdes and Happee 1994). Indeed, the use of neural nets to perform correlation in the CCS and to implement a new SP predictor has been proposed, to increase flexibility and decrease simulation time of the model.

*Acknowledgements.* This work was supported by grants from the Human Frontier Science Program. The authors would like to thank Gabriel Gauthier, Jean Blouin and Thelma Coyle for helpful comments during the preparation of the manuscript. Stefano Lazzari was a Ph.D. student from the University of Pavia, Italy, and was supported by a fellowship from the Politecnico di Milano.

## References

Angel RW, Garland H (1972) Transfer of information from manual to oculomotor control system. J Exp Psychol 96: 92–96

Bahill AT, McDonald JD (1983) Model emulates human smooth pursuit system producing zero-latency target tracking. Biol Cybern 48: 213–222

Bahill AT, Stark L (1979) The trajectories of saccadic eye movements. Sci Am 240: 108–117

Becker W (1989) Metrics. In: Wurtz R, Goldberg M (eds) The neurobiology of saccadic eye movements. Elsevier, Amsterdam, pp 13–67

Becker W, Jurgens R (1979) An analysis of the saccadic system by means of double step stimuli. Vision Res 19: 967–983

Bock O (1987) Coordination of arm and eye movements in tracking of sinusoidally moving targets. Behav Brain Res 24: 93–100

Buizza A, Schmid R (1986) Velocity characteristics of smooth pursuit eye movements to different patterns of target motion. Exp Brain Res 63: 395–401

Buizza A, Schmid R (1989) Influence of smooth pursuit dynamics on eye tracking: a mathematical approach. Med Biol Eng Comput 27: 617–622

Buizza A, Leger A, Berthoz A, Schmid R (1979) Otolithic-acoustic interaction in the control of eye movement. Exp Brain Res 36: 509–522

Cordo P, Carlton L, Bevan L, Carlton M, Kerr GK (1994) Proprioceptive coordination of movement sequences: role of velocity and position information. J Neurophysiol 71: 1848–1861

Craik KJW (1947) Thory of human operator in control systems. I. The operator as an engineering system. Br J Psychol 38: 56–61

Gauthier GM, Hofferer JM (1976a) Eye tracking of self-moved targets in absence of vision. Exp Brain Res 26: 121–139

Gauthier GM, Hofferer JM (1976b) Eye movements in response to real and apparent motions of acoustic targets. Percept Mot Skills 42: 963–971

Gauthier GM, Mussa Ivaldi F (1988) Oculo-manual tracking of visual targets in monkey: role of the arm afferent information in the control of arm and eye movements. Exp Brain Res 73: 138–154

Gauthier GM, Vercher J-L, Mussa Ivaldi F, Marchetti $E$ (1988) Oculo-manual tracking of visual targets: control learning, coordination control and coordination model. Exp Brain Res 73: 127–137

Gerdes VGJ, Happee R (1994) The use of an internal representation in fast goal-directed movements: a modelling approach. Biol Cybern 70: 513–524

Jones LA, Hunter IW (1990) Influence of the mechanical properties of a manipulandum on human operator dynamics. Biol Cybern 62: 299–307

Jurgens R, Becker W, Kornhuber HH (1981) Natural and drug-induced variations of velocity and duration of human saccadic eye movements: evidence for a control of the neural pulse generator by local feedback. Biol Cybern 39: 87–96

Kawano K, Watanabe Y, Kaji S, Yamane S (1990) Neuronal activity in the posterior parietal cortex and pontine nucleus of alert monkey during ocular following responses. In: Iwai E, Mishkin M (eds) Vision, memory and the temporal lobe. Elsevier, Amsterdam, pp 311–315

Knapp HD, Taub E, Berman AJ (1963) Movements in monkeys with deafferented forelimbs. Exp Neurol 7: 305–315

Lamarre Y, Bioulac B, Jacks B (1978) Activity of precentral neurones in conscious monkeys: effects of deafferentation and cerebellar ablation. J Physiol (Paris) 74: 253–264

Lamarre Y, Busby L, Spidalieri G (1983) Fast ballistic arm movements triggered by visual, auditory, and somesthetic stimuli in the monkey. I. Activity of precentral cortical neurons. J Neurophysiol 50: 1343–1358

Meyer CH, Lasker AG, Robinson DA (1985) The upper limit of human smooth pursuit velocity. Vision Res 25: 561–563

Miall RC, Weir DJ, Stein JF (1985) Visuomotor tracking with delayed visual feedback. Neuroscience 16: 511–520

Miall RC, Weir DJ, Stein JF (1988) Planning of movement parameters in a visuo-motor tracking task. Behav Brain Res 17: 1–8

Miall RC, Weir DJ, Stein JF (1993) Intermittency in human manual tracking tasks. J Mot Behav 25: 53–63

Navas SI, Stark L (1968) Sampling or intermittency in hand control system dynamics. Biophys J 8: 252–302

Newsome WT, Wurtz RH, Komatsu H (1988) Relation of cortical area MT and MST to pursuit eye movements. II. Differentiation of retinal from extraretinal inputs. J Neurophysiol 60: 604–620

Rashbass C (1961) The relationship between saccadic and smooth tracking eye movements. J Physiol (Lond) 159: 326–338

Robinson DA (1975) Oculomotor control signals. In: Lennerstrand G, Bach-y-Rita P (eds) Basic mechanisms of ocular motility and their clinical implications. Pergamon Press, New York, pp 337–374

Robinson DA, Keller EL (1972) The behavior of eye movement motoneurons in the alert monkey. Bibl Ophtalmol 82: 716–720

Robinson DA, Gordon JL, Gordon SE (1986) A model of the smooth pursuit eye movement system. Biol Cybern 55: 43–57

Sittig AC, Denier van der Gon JJ, Gielen CCAM (1985) Separate control of arm position and velocity demonstrated by vibration of muscle tendon in man. Exp Brain Res 60: 445–453

Stein JF, Miall RC, Weir DJ (1987) Role of the cerebellum in the visual guidance of movement. In: Glickstein M, Yeo C, Stein JF (eds) Cerebellum and neuronal plasticity. Plenum Press, New York, pp 175–191

Steinbach MJ (1969) Eye tracking of self-moved targets: the role of efference. J Exp Psychol 82: 366–376

Suzuki DA, Keller EL (1988) The role of the posterior vermis of monkey cerebellum in smooth-pursuit eye movement control. II. Target velocity-related Purkinje cell activity. J Neurophysiol 59: 19–40

van Gisbergen JAM, Robinson DA, Gielen S (1981) A quantitative analysis of generation of saccadic eye movements by burst neurons. J Neurophysiol 45: 417–422

Vercher JL, Gauthier GM (1992) Oculo-manual coordination control: ocular and manual tracking of visual targets with delayed visual feedback of the hand motion. Exp Brain Res 90: 599–609

Vercher JL, Volle M, Gauthier GM (1993) Dynamics of human visuo-oculo-manual coordination control in target tracking tasks. Aviat Space Environ Med 64: 500–506

Vercher JL, Quaccia D, Gauthier GM (1995) Oculo-manual coordination control: respective role of visual and non-visual information in ocular tracking of self-moved targets. Exp Brain Res 103: 311–322

Vercher JL, Gauthier GM, Blouin J, Guédon O, Cole J, Lamarre Y (1996) Oculo-manual tracking in normal subjects and a deafferented patient: respective role of arm motor efference and proprioception in initiation of smooth pursuit of self-moved targets. J Neurophysiol 76: 1133–1144

Vercher JL, Lazzari S, Gauthier GM (1997) Manuo-ocular coordination in target tracking. II. Comparing the model with human behavior. Biol Cybern 77, 267–275

Westheimer G (1954) Mechanism of saccadic eye movements. AMA Arch Ophtalmol 52: 720–724

Wolpert D, Miall RC, Winter JL, Stein JF (1992) Evidence for an error deadzone in compensatory tracking. J Mot Behav 24: 299–308

Young LR (1971) Pursuit eye tracking movements. In: Bach-y-Rita P, Collins CC, Hyde JE (eds) The control of eye movements. Academic Press, New York, pp 429–443

Young LR (1981) The sampled data model and foveal deadzone for saccades. In: Zuber BL (ed) Models of oculomotor behavior and control. CRC Press, Boca Raton, pp 43–74

Young LR, Stark L (1962) A sampled data model for eye-tracking movements. Q Prog Rep Res Lab Electr MIT 66: 370–384

Zee DS (1986) Brain stem and cerebellar deficits in eye movement control. Trans Am Ophthalmol Soc 105: 599–605